SCIENCE CHINA
Information Sciences

• LETTER •

February 2026, Vol. 69, Iss. 2, 129401:1–129401:2
https://doi.org/10.1007/s11432-025-4514-x

Physical structure-based small signal modeling for GaN Fin-HEMTs

Ziyue ZHAO, Yang LU*, Chupeng YI, Ting FENG, Xin LIU, Wei ZHAO, Guanghai YAO, Yilin CHEN*, Xiaohua MA & Yue HAO

National Engineering Research Center of Wide Band-gap Semiconductor, Xidian University, Xi'an 710071, China

Received 11 January 2025/Revised 22 March 2025/Accepted 2 July 2025/Published online 22 October 2025

Citation Zhao Z Y, Lu Y, Yi C P, et al. Physical structure-based small signal modeling for GaN Fin-HEMTs. Sci China Inf Sci, 2026, 69(2): 129401, https://doi.org/10.1007/s11432-025-4514-x

Gallium nitride (GaN) high electron mobility transistors (HEMTs) have been extremely attractive in high-power, high-voltage, and high-frequency fields due to their many merits, including high power output, high operating frequency, and high breakdown electric field. Benefiting from their advanced tri-gate structure, Fin-HEMTs can significantly enhance gate control and effectively suppress device performance degradation caused by short-channel effects (SCEs) [1]. The structure of the Fin-HEMT is shown in Figure 1(a), which exhibits a periodic nanochannel structure by using the etching process.

The small signal model (SSM) of a device not only characterizes the structural characteristics, but also serves as the foundation for the large signal model, which is a link between the device and the circuit [2].

A physical structure-based SSM (named PS-model) and a parameter extraction method of Fin-HEMTs were proposed. Firstly, in this model, the parasitic gate capacitance (C_g) between the gate and the two-dimensional electron gas (2DEG) was taken into account, which is calculated using simulation techniques and conformal transformations. Secondly, the capacitance between the trench region and the 2DEG was introduced in the PS-model, incorporating parallel capacitors, namely C_{gs_trench} and C_{gd_trench}.

Results and discussion. The electron concentration distribution was simulated by using Silvaco TCAD in order to isolate the control ability of the side-wall gate. The performance of the device with three different W_{Fin} (200, 250, 300 nm) was simulated. Figures 1(b)–(d) show the electron concentration distribution of Fin-HEMTs with W_{Fin} of 200, 250, 300 nm respectively, under a gate voltage (V_{gs}) and drain voltage (V_{ds}) of 0 V. It can be found that the Schottky contact of the side-wall gate can effectively deplete the 2DEG in the channel along the Fin width direction, assisting the top-gate to control the carrier in the channel, and improve the control ability of the whole gate. Figure 1(e) shows the electron concentration distribution of cross sections along the W_{Fin} (200, 250, 300 nm) at the heterojunction interface, which reflects the influence of the side-wall gate on the carrier concentration. The electron concentration distribution in Figure 1(e) can be divided into three regions along the width direction of the gate.

For the Fin-HEMTs, side-wall gates induce a more pronounced C_g. At the same time, the parasitic capacitances are also generated between the trench region and 2DEG, which affects C_{gs} and C_{gd} directly. Therefore, in order to build an accurate Fin-HEMT model, it is necessary to consider the influence of C_g and the trench region.

The formula of the C_{g_top} is shown in (1). C_{g_side} is calculated by (2)–(4). Where $K(x)$ represents the complete elliptic integral of the first class, which can be calculated rapidly by MATLAB R2023a. And $K'(x) = K(x')$, x' represents the complementary modulus of x [3, 4]. The formula for x' is shown in (5). The total C_g is determined by the W_g and the Fin period ($W_{Fin}+W_{trench}$) which is calculated by (6).

For the trench region, the gate shows a vertical relationship with 2DEG. The capacitance between the gate in the trench region and the 2DEG can be calculated by the above method. The top view of the device is shown in Figure 1(f). The capacitance between the trench region and the 2DEG in the gate-source region is defined as C_{gs_trench}, and the capacitance between the trench region and the 2DEG in the gate-drain region is defined as C_{gd_trench}.

$$C_{g\_top} = \varepsilon_{AlGaN} \frac{L_g \times W_{top}}{T_{AlGaN}}, \tag{1}$$

$$\begin{aligned}\frac{C_{g\_side}}{L_g} = {} & \varepsilon_{AlGaN} \left[\frac{K'(k_{up\_in})}{K(k_{up\_in})} + \frac{K'(k_{up\_out})}{K(k_{up\_out})}\right] \\ & + \varepsilon_{GaN} \left[\frac{K'(k_{down\_in})}{K(k_{down\_in})} + \frac{K'(k_{down\_out})}{K(k_{down\_out})}\right],\end{aligned} \tag{2}$$

$$k_{up\_in} = \frac{T_{ox}}{T_{ox}+W_{side}} \sqrt{\frac{(T_{ox}+W_{side})^2 + T_{AlGaN}^2}{T_{ox}^2 + T_{AlGaN}^2}}, \tag{3}$$

$$k_{up\_out} = \sqrt{\frac{T_{ox}^{2/3}((T_{ox}+W_{side})^{2/3} + T_{AlGaN}^{2/3})}{(T_{ox}+W_{side})^{2/3}(T_{ox}^{2/3} + T_{AlGaN}^{2/3})}}, \tag{4}$$

$$x' = \sqrt{1-x^2}, \tag{5}$$

$$C_g = (C_{g\_top} + 2 \times C_{g\_side}) \times \left(\frac{W_g}{W_{Fin}+W_{trench}}\right). \tag{6}$$

The PS-model is established based on the physical structure of

* Corresponding author (email: luyang@xidian.edu.cn, chenyilin@xidian.edu.cn)

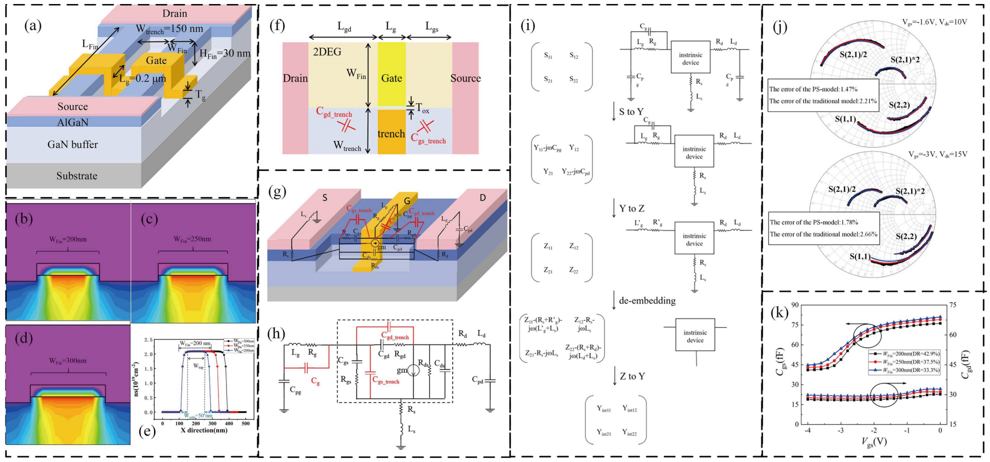

Figure 1 (Color online) (a) The structure of the GaN Fin-HEMTs; (b)–(d) the electron concentration distribution of Fin HEMTs with W_{Fin} of 200, 250, 300 nm, respectively, at gate voltage and drain voltage of 0 V; (e) the electron concentration distribution of cross sections along the W_{Fin} (200, 250, 300 nm) at the heterojunction interface of the device; (f) the top view of the device in a cycle and the relationship of the C_{gs_trench} and the C_{gd_trench}; (g) the stereogram of the device in a cell and the structure of the SSM; (h) the equivalent circuit topology of the GaN Fin-HEMT, which is called PS-model; (i) the method for extracting the device intrinsic Y matrix; (j) the fitting result of the PS-model under (−1.6 V, 10 V) and (−3 V, 15 V), black curves represent the measured S-parameters, red curves represent the S-parameters fitting results using the PS-model, and blue curves represent the fitting results using the traditional GaN HEMT model in [5]. The frequency range for the S-parameters is 1–30 GHz, and the testing step is 0.1 GHz; (k) comparison of the C_{gs} and C_{gd} among the Fin-HEMTs with 200 nm Fin width, 250 nm Fin width, and 300 nm Fin width.

the Fin-HEMT, and the structure of the model is shown in Figure 1(g). The equivalent circuit topology (the PS-model) of the device is shown in Figure 1(h). In the model shown in Figure 1(h), the parameters inside the dotted line are intrinsic parameters, and the others are parasitic parameters.

Due to the introduction of C_g, the de-embedding method is different from the traditional way, which is represented by Figure 1(i). It is worth noting that in order to simplify the calculation, the parallel structure composed of C_g, R_g, and L_g needs to be equivalent to the series structure of L'_g and R'_g. The calculation method of the parameters is shown as (7)–(11).

$$R'_g = a/c, \tag{7}$$

$$L'_g = b/c, \tag{8}$$

$$a = R_g(R_g^2 + \omega^2 L_g^2), \tag{9}$$

$$b = (R_g^2 + \omega^2 L_g^2)(C_g R_g^2 - L_g + \omega^2 C_g L_g^2), \tag{10}$$

$$c = R_g^2 + \omega^2 (C_g R_g^2 - L_g + \omega^2 C_g L_g^2)^2. \tag{11}$$

After the calculation and extraction of model parameters, the model has been able to achieve an ideal fit in this work. Taking biases (−1.6 V, 10 V) and (−3 V, 15 V) as examples, the fitting results are shown in Figure 1(j). In order to express the advancement of the PS-model more directly, the fitting results of the PS-model are also compared with those of the traditional model [5] in Figure 1(j).

C_{gs} and C_{gd} of devices with different Fin widths are analyzed in Figure 1(k). The C_{gs} and C_{gd} gradually increase with the increase of V_{gs}. As the Fin width decreases, the overall trend of C_{gs} and C_{gd} is increasing. It has been proven that the gate capacitance increases with the decrease in W_{Fin} due to the improved side-wall gate control in narrower Fin structures.

Conclusion. In this work, a novel SSM (PS-model) for GaN Fin-HEMT is established. Based on the physical structure of the device, the PS-model introduces three new model parameters, C_g, C_{gs_trench}, and C_{gd_trench}, which are used to represent the capacitance generated between the Fin structure and 2DEG. Because the new parameters have specific physical significance, parameter values can be calculated by the conformal transformation, which can quickly obtain parameter values and improve the efficiency and accuracy of model establishment. Finally, the PS-model can accurately fit the S-parameter of GaN Fin-HEMTs, and the fitting accuracy is better than 98%.

Acknowledgements This work was supported by Fundamental Research Funds for the Central Universities (Grant Nos. XJSJ23053, XJSJ23052, ZYTS23026, XJS221113) and National Natural Science Foundation of China (Grant Nos. 62234009, and 62090014).

Supporting information Appendix A. The supporting information is available online at info.scichina.com and link.springer.com. The supporting materials are published as submitted, without typesetting or editing. The responsibility for scientific accuracy and content remains entirely with the authors.

References

1 Im K S, Won C H, Jo Y W, et al. High-performance GaN-based nanochannel FinFETs with/without AlGaN/GaN heterostructure. IEEE Trans Electron Devices, 2013, 60: 3012–3018
2 Huang F Y, Tang X S, Wei Z N, et al. An improved small-signal equivalent circuit for GaN high-electron mobility transistors. IEEE Electron Device Lett, 2016, 37: 1399–1402
3 Xiang Y. Further study on electrostatic capacitance of an inclined plate capacitor. J Electrostatics, 2008, 66: 366–368
4 Sruthi M P, Shanbhag A, Nair D R, et al. Scalable charge-based compact model for drain current in fin-shaped GaN HEMTs. IEEE Trans Electron Devices, 2023, 70: 979–985
5 Zhao Z, Lu Y, Yi C, et al. A fast small signal modeling method for GaN HEMTs. Solid-State Electron, 2021, 175: 107946